Inst. Metal Finish., **69,** 140 (1991).
6. M. Schwartz and G. O. Mallory, *J. Electrochem. Soc.*, **123,** 606 (1976).
7. V. Morton and R. D. Fisher, *J. Electrochem. Soc.*, **116,** 188 (1969).
8. P. A. Albert, Z. Kovac, H. R. Lilienthal, T. R. McGuire, and Y. Nakamura, *J. Appl. Phys.*, **38,** 1258 (1967).
9. K. Miyoshi and K. Harada, *J. Met. Finish. Soc. Jpn.*, **28,** 522 (1977).
10. T. Osaka, H. Sawai, F. Otoi, and K. Nihei, *J. Met. Finish. Soc. Jpn.*, **31,** 661(1980).
11. T. Osaka, H. Sawai, and N. Kasai, *J. Met. Finish. Soc. Jpn.*, **32,** 615 (1981).
12. S. T. Pai, J. P. Marton, and J. D. Brown, *J. Appl. Phys.*, 43, 282 (1972).
13. T. Osaka, M. Fukawa, and J. Kawaguchi, *Denki Kagaku oyobi Kogyo Butsuri Kagaku*, **60,** 523 (1992).
14. I. Nakayama, M. Fukawa, T. Homma, and T. Osaka, *J. Surf. Finish. Soc. Jpn.*, **43,** 835 (1992).
15. I. Koiwa, M. Usuda, and T. Osaka, *J. Electrochem. Soc.*, **135,** 1222 (1988).
16. I. Koiwa, M. Usuda, K. Yamada, and T. Osaka, *J. Electrochem. Soc.*, **135,** 718 (1988).
17. A. Iizuka, T. Higashikawa, and T. Osaka, in *Electrochemically Deposited Thin Films III,* M. Paunovic and D. A. Scherson, Editors, PV 96-19, p. 184, The Electrochemical Society Proceedings Series, Pennington, NJ (1996).
18. T. Hatsukawa, T. Higashikawa, T. Osaka, and H. Nakao, *J. Surf. Finish. Soc. Jpn.*, **47,** 779 (1996).
19. K. Masui, S. Maruno, and T. Yamada, *J. Jpn. Inst. Met.*, **41,** 1130 (1977).
20. T. Osaka and I. Koiwa, *J. Met. Finish. Soc. Jpn.*, **34,** 330 (1983).

Prediction of Li Intercalation and Battery Voltages in Layered vs. Cubic Li_xCoO_2

C. Wolverton and Alex Zunger

National Renewable Energy Laboratory, Golden, Colorado 80401, USA

ABSTRACT

It is now possible to use a quantum-mechanical electronic structure theory of solids and derive, completely from "first-principles," the voltage of a battery based on intercalation reaction energetics. Using such techniques, we investigate the structural stability, intercalation energies, and battery voltages of the two observed ordered phases ("layered" and cubic) of $LiCoO_2$. We perform calculations for not only fully lithiated $LiCoO_2$, but also fully delithiated $\square CoO_2$ and partially delithiated $Li_{0.5}CoO_2$. Our calculations demonstrate that removal of Li from the cubic phase results in movement of the Li atoms from their original octahedral sites to tetrahedral sites, forming a low-energy $LiCo_2O_4$ spinel structure. The energetics of the spinel phase are shown to account for the observed marked differences in battery voltages between the cubic and layered phases of $LiCoO_2$. A small energy barrier exists for Li motion between octahedral and tetrahedral sites, thus indicating the metastability of the high-energy octahedral sites. Finally, we point out a possible pressure-induced layered → cubic transition in $LiCoO_2$.

Introduction

Li_xCoO_2 is used as a positive electrode (cathode) material in rechargeable Li batteries, in which Li is intercalated into and out of the structure.[1-3] Hence, Li_xCoO_2 can exist in a range of Li compositions x. The starting material $LiCoO_2$ ($x = 1$) has been synthesized in two ordered forms (see Fig. 1). There is a "layered" rhombohedral form which can be synthesized at high temperatures (~800°C),[1-7,12,13] which we also call "CuPt-like" (because the cations, Li and Co, form the CuPt structure also analogous to cations in the ordered $GaInP_2$ structure; see, e.g., Ref. 14 or 15) and a cubic form which has been produced by solution growth at low temperatures (~400°C).[8-11,16-18] We also refer to this latter form as "D4."[19] The cubic form of $LiCoO_2$ is sometimes referred to in the literature as "low-temperature $LiCoO_2$," but there is still some uncertainty about the exact degree and nature of ordering in this compound. Because the cubic phase is synthesized at low temperature, it is likely to be less perfectly ordered than the high temperature synthesized layered CuPt phase. Thus, we refer to the perfectly ordered cubic structure shown in Fig. 1 as D4, and note that the actual low temperature synthesized phase may be some partially ordered version of D4. Layered CuPt and cubic D4 are extremely similar in terms of atomic coordination sequence. Pair and three-body correlations are equivalent, with the first difference between the two occurring at the four-body correlation.[19,20] Thus, one would expect the two forms of Li_xCoO_2 to exhibit similar energies and electrochemical potentials. However, electrochemical properties of the two compounds are very different. When used as a cathode material in Li_xCoO_2/Li cells, the cubic D4 structure has a nearly flat voltage plateau at 3.6 V (for $1/2 \lesssim x \lesssim 1$), which contrasts with the voltage profile of layered CuPt which takes place mostly above 4 V and has many voltage drops and plateaus. This distinction is initially difficult to understand given the structural similarity between the two and the expected similar stability. Two possible explanations could be offered for this unexpected distinction. (*i*) First, despite the similarities in the nominal (i.e., undistorted) layered CuPt and cubic D4 structures, the differences in symmetry between the two results in different structural distortions, that is, CuPt is a layered LiO/CoO superlattice along the [111] direction, whereas the cubic D4 structure is not a superlattice. Thus, the layered CuPt structure has one extra structural degree of freedom (namely, a c/*a* ratio) that the D4 structure lacks. To the extent that $R_{Li} \neq R_{Co}$, the layered nature of the CuPt phase will distort the Li-Co interplanar distances from their ideal values, thereby changing both relative total energies and the X-ray diffraction pattern (e.g., splitting and shifting of peaks) in a measurable way. (*ii*) Another possibility for the electrochemical distinction between CuPt and D4 is that the structures of these two compounds could change with Li composition x, and correspondingly, relative stability between the two phases might change.

It has recently become possible to relate the average cell (battery) potential of an intercalation reaction to the quantum-mechanically calculated heat of reaction.[21,22] In turn, the calculated heat of reaction is sensitive to the structure of the reactants. Thus, a direct link exists via quantum-mechanical total energy calculations between crystal structure and battery potential. Using such techniques, we study the two possibilities (*i*) and (*ii*) to ascertain the structural and electrochemical properties (i.e., Li intercalation energies) of the two compounds. To do so, we study relax-

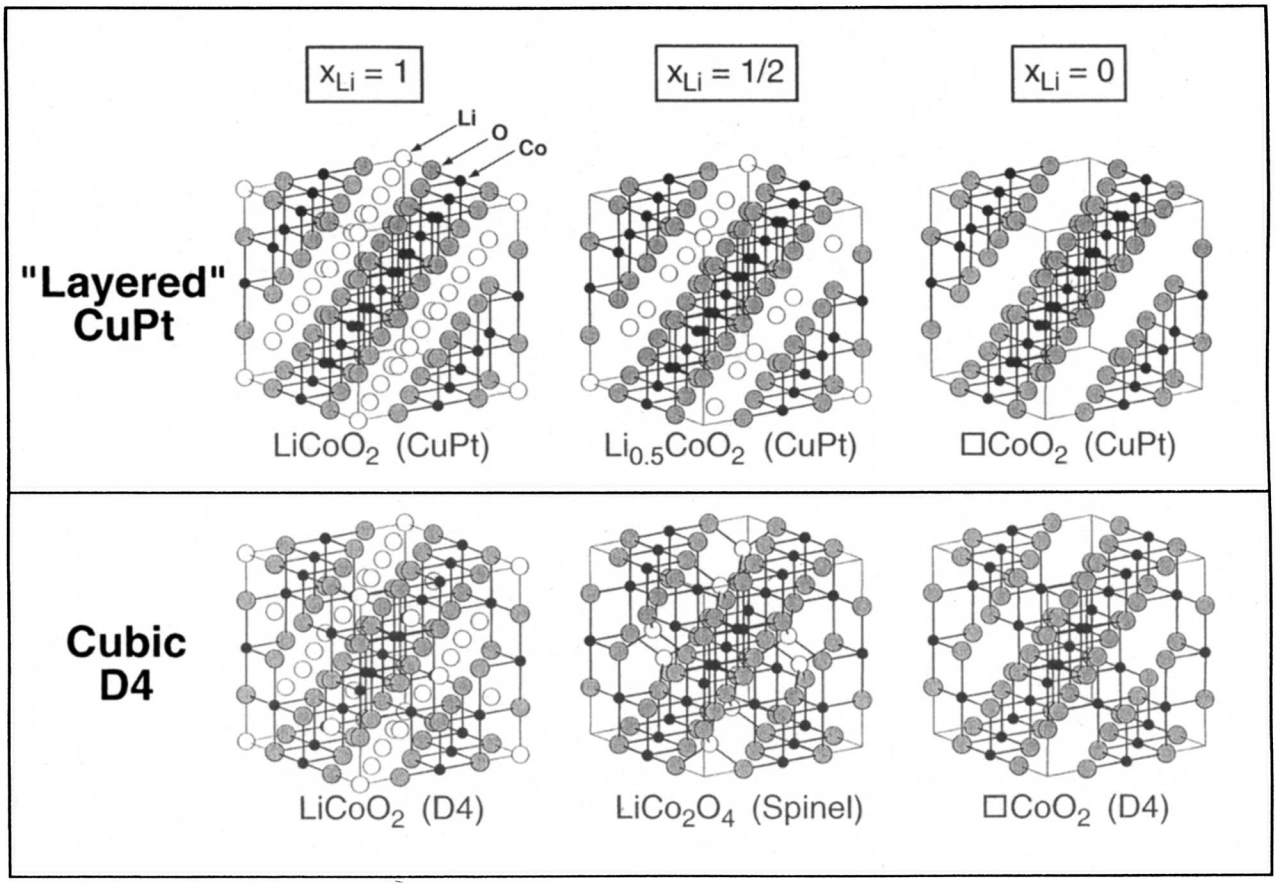

Fig. 1. The CuPt and D4 structures of Li_xCoO_2 for $x = 1$, 1/2, and 0. Li, Co, and O atoms are shown as large white, small black, and large gray circles, respectively.

ation in the two structures, and also explore "derivative Li_xCoO_2 structures" for intermediate compositions $x \neq 0, 1$ using "state-of-the-art" electronic structure techniques.[23] We also look for possible transition paths (e.g., external pressure) connecting the two ordered phases.

The summary of our calculated results are (*i*) the calculated *c*/*a* ratio of layered $LiCoO_2$ (4.84) is close to ideal ($2\sqrt{6} = 4.90$); consequently, $LiCoO_2$ in the layered CuPt and cubic D4 structures are energetically nearly degenerate. (*ii*) Upon removal of Li, the *c*/*a* ratio in $\square CoO_2$ (CuPt) decreases dramatically, whereas no such distortion occurs for $\square CoO_2$ (D4). Thus, the small energy difference between CuPt and D4 is amplified by more than a factor of ten upon removal of Li. (*iii*) Due to points (*i*) and (*ii*), the voltage of Li_xCoO_2/Li cells, averaged over all Li compositions, is larger for a cathode with the cubic D4 structure compared with the layered CuPt structure. This is in contrast with electrochemical measurements which show a lower voltage for D4. (*iv*) However, via removal of Li from the cubic D4 structure, the Li atoms move from octahedral to tetrahedral sites and form a new structure: the low energy normal spinel compound, $LiCo_2O_4$. The low energy of this compound explains the low voltage of the cubic structure relative to layered CuPt (for $x \gtrsim 0.5$). (*v*) For $0 < x < 0.5$, we predict the average voltage of the D4 should rise significantly upon removal of Li from the tetrahedral sites in $LiCo_2O_4$. (*vi*) A small energy barrier is shown to exist between Li in the T_d and O_h sites in $LiCoO_4$, thus demonstrating that the octahedral sites in the cubic phase are metastable. (*vii*) We point out a possible pressure-induced transition between the layered and cubic structures of $LiCoO_2$.

Structural Properties of Layered CuPt and Cubic D4 Forms of $LiCoO_2$

The two main structures considered here for $LiCoO_2$ are the layered CuPt and cubic D4 structures as shown in Fig. 1. Structural information for CuPt and D4 is given in Table I. The CuPt structure is rhombohedral, a superlattice in the [111] direction, and has space group $R\bar{3}m$, whereas the D4 structure is face-centered cubic (fcc), is not a superlattice, and has space group $Fd3m$.[a] The primitive cell vectors are given in Table I, but these phases are often depicted in terms of their conventional cells. The CuPt phase can be mapped onto a set of hexagonal axes (as can any rhombohedral cell) which has three times the volume of the primitive cell. One should note that this does not imply that the symmetry of the phase is hexagonal, as sometimes asserted in the literature. The conventional D4 cell is a cubic cell which has four times the volume of the primitive cell. Both structures (when undistorted) contain an fcc sublattice of oxygen anions. The Li and Co cations occupy all the octahedral O_h sites of this anion sublattice; the tetrahedral T_d sites are completely unoccupied.

The structural degrees of freedom between CuPt and D4 differ. Naturally, both phases have the degree of freedom associated with changes in the unit cell volume. However, the CuPt phase has an additional cell-external distortion (δ of Table I which corresponds to a *c*/*a* ratio for the conventional cell) allowed by symmetry which the D4 phase lacks. In addition, both phases have cell-internal degrees of freedom (*z* of Table I) associated with the fact that the location of the oxygen atoms within both the CuPt or D4 cells is not fixed by the point symmetry of their Wyckoff

[a] From Fig. 1, one might suppose that the D4 structure could be described as a [111] superlattice with one-quarter of the Li atoms on Co sites and vice versa. Hence, the D4 structure could be described as the CuPt structure with partial long-range order. However, such a description would be misleading: the "anti-sited" atoms are not placed at random, but rather are in an ordered array such that the symmetry of the structure is cubic, and the anti-sited atoms are, in fact, symmetry-equivalent to the other atoms. (Each Li atom is in a Co-rich plane in one of the four possible [111] directions, but is in a Li-rich plane in each of the other three [111] directions.) Thus, such a description of D4 is not particularly useful.

Table I. Structural information for the octahedrally coordinated $LiCoO_2$ phases: layered CuPt and cubic D4. Both primitive and conventional cell vectors are given. Only the atomic positions of symmetrically distinct atoms are given. The ideal values of structural parameters are given by atoms in ideal undistorted rocksalt positions.

	"Layered" CuPt	Cubic D4
Bravais lattice	Rhombohedral	Face-centered cubic
Space group	$R\bar{3}m$	$Fd3m$
Superlattice	LiO/CoO along [111]	None
Primitive translation vectors	$\mathbf{a}_1 = a'[1, \alpha, 1]$ $\mathbf{a}_2 = a'[1, 1, \alpha]$ $\mathbf{a}_3 = a'[\alpha, 1, 1]$ $\alpha = \frac{4 + 2\delta}{4 - \delta}$	$\mathbf{a}_1 = \frac{a}{2}[0, 1, 1]$ $\mathbf{a}_2 = \frac{a}{2}[1, 0, 1]$ $\mathbf{a}_3 = \frac{a}{2}[1, 1, 0]$
Atoms/primitive cell	4	16
Conventional translation vectors	$\mathbf{c} = \mathbf{a}_1 + \mathbf{a}_2 + \mathbf{a}_3;\ c = \lvert\mathbf{c}\rvert = a'\frac{12\sqrt{3}}{4 - \delta}$ $\mathbf{a} = \mathbf{a}_1 - \mathbf{a}_2;\ a = \lvert\mathbf{a}\rvert = a'\frac{3\sqrt{2}\delta}{4 - \delta}$	$a = \lvert\mathbf{a}\rvert = \lvert\mathbf{a}_1 + \mathbf{a}_2 - \mathbf{a}_3\rvert$
Atomic positions (in units of $\mathbf{a}_i$)	$\tau_{Li} = (0, 0, 0)$ $\tau_{Co} = \left(\frac{1}{2}, \frac{1}{2}, \frac{1}{2}\right)$ $\tau_O = (z, z, z)$	$\tau_{Li} = (0, 0, 0)$ $\tau_{Co} = \left(\frac{1}{2}, \frac{1}{2}, \frac{1}{2}\right)$ $\tau_O = (z, z, z)$
Bond lengths	$R_{Li-O} = \frac{a'\sqrt{6}}{4 - \delta}\sqrt{72z^2 - 48z + \delta^2 + 8}$ $R_{Co-O} = \frac{a'\sqrt{6}}{4 - \delta}\sqrt{72z^2 - 24z + \delta^2 + 2}$	$R_{Li-O} = \frac{a}{2}\sqrt{12z^2 - 4z + \frac{1}{2}}$ $R_{Co-O} = \frac{a}{2}\sqrt{12z^2 - 8z + \frac{3}{2}}$
Cell distortions	$\delta = \frac{c/a_{ideal}}{c/a}$	None
Ideal parameters	$\delta^0 = 1;\ z^0 = \frac{1}{4}$	$z^0 = \frac{1}{4}$
Undistorted bond lengths	$R^0_{Li-O} = R^0_{Co-O} = a'$	$R^0_{Li-O} = R^0_{Co-O} = a/4$
Calculated parameters	$\delta = 0.99;\ z = 0.262$	$z = 0.259$
Calculated bond lengths	$R_{Li-O} = 2.08$ Å; $R_{Co-O} = 1.90$ Å	$R_{Li-O} = 2.05$ Å; $R_{Co-O} = 1.91$ Å

positions. To specify the positions of the oxygen atoms, one requires an additional cell-internal parameter, z. The undistorted value of this parameter is $z^0 = 1/4$, which leads to equal Li–O and Co–O bond lengths. For $z \neq z^0$, the two nearest-neighbor bond lengths are distinct: $R_{Li-O} \neq R_{Co-O}$. Expressions for these bond lengths in terms of z and cell vectors are given in Table I. For both structures, every nearest-neighbor Li–O bond is equivalent by symmetry, and similarly for Co–O bonds. In lower symmetry structures, the equivalence of these bonds may be broken, leading to several different types of Li–O or Co–O bonds.

Quantum-Mechanical Calculation of Battery Voltage and Structural Stability

For Li_xCoO_2 in the structure σ (= CuPt or D4), the heat of the Li battery intercalation reaction between two Li compositions x_1 and x_2 is given by

$$\Delta H^{\sigma}_{react}(x_2, x_1) = E_{tot}(Li_{x_2}CoO_2, \sigma) - E_{tot}(Li_{x_1}CoO_2, \sigma) - (x_2 - x_1)E_{tot}(Li, bcc) \quad [1]$$

E_{tot} is the total energy of a system of electrons in the Coulomb potential due to the nuclei. $\Delta H^{\sigma}_{react}$ is the energy gained upon deintercalation of Li from $LiCoO_2$, relative to Li metal. This intercalation reaction energy is simply related to the (zero temperature and pressure) open-circuit average battery voltage of a Li_xCoO_2/Li cell between the intercalation compositions x_2 and x_1 (see, e.g., Ref. 24 or 22)

$$\overline{V}(\sigma, x_2, x_1) = \int_{x_1}^{x_2} dx\, V(x) = \frac{-\Delta H^{\sigma}_{react}(x_2, x_1)}{F(x_2 - x_1)} \quad [2]$$

where F is the Faraday constant. Therefore, by computing the energetics of Li intercalation in Eq. 1 we ascertain the average battery voltage.

We use density functional theory[25] within the local density approximation[26] (LDA) to obtain the total energies E_{tot} of various Li_xCoO_2 structures in Eq. 1 and hence the average of voltages of Eq. 2. The total energy of electrons plus nuclei is given by

$$E_{tot} = \sum_i \epsilon_i - \frac{1}{2}\iint \frac{\rho(\mathbf{r})\rho(\mathbf{r}')}{|\mathbf{r} - \mathbf{r}'|} d^3\mathbf{r} d^3\mathbf{r}' + E_{xc}[\rho(\mathbf{r})] - \int \rho(\mathbf{r}) V_{xc}[\rho(\mathbf{r})] d^3\mathbf{r} + \frac{1}{2}\sum_{\alpha\beta} \frac{Z_\alpha Z_\beta}{|\mathbf{R}_\alpha - \mathbf{R}_\beta|} \quad [3]$$

The terms, are respectively, the sum of one-electron eigenvalues (up to the Fermi level), the electron-electron Coulomb energy, the exchange-correlation energy, the term involving the exchange-correlation potential, V_{xc}, and the ion-ion Coulomb energy. We first assume a set of atomic positions $\{R_\alpha\}$ (including unit cell parameters, Table I) and solve, for it, the Schrödinger equation

$$\hat{H}(\{R_\alpha\})|\Psi\rangle = \epsilon_i(\{R_\alpha\})|\Psi\rangle \quad [4]$$

where $\hat{H}$ is the electron-electron, electron-ion, and ion-ion Hamiltonian. This produces the electronic charge density

$\rho(\mathbf{r}) = \Sigma_i \Psi_i^* \Psi_i$, and eigenvalues ϵ_i. These are used to evaluate the total energies of Eq. 3. The procedure is repeated for different structural parameters until E_{tot} is minimized, or equivalently until the quantum-mechanically calculated forces vanish.

To solve the Schödinger equation and evaluate E_{tot}, we have used the full potential LAPW[23] method. We thus determined the relaxed geometries and total energies for Li_xCoO_2 in the CuPt and D4 structures. We used the exchange correlation of Ceperley and Alder,[27] as parameterized by Perdew and Zunger.[28] LAPW sphere radii were chosen to be 2.0, 2.0, and 1.3 a.u. for Li, Co, and O, respectively. A well-converged basis set was used, corresponding to an energy cutoff of 25.5 Ry ($RK_{max} = 6.57$). For most calculations, Brillouin-zone integrations were performed using the equivalent k point sampling method.[29] For some structures not simply related to the CuPt or D4 structures by substitutional changes, the method of special k points was used. (All calculations were estimated to be converged with respect to k points to within 1 mRy/cell.) All total energies were optimized with respect to all degrees of freedom (volume as well as all cell-internal and cell-external coordinates). Spin polarization only had a small effect on the energy of these compounds[30]; hence, the calculations below for the energetics of cation ordering were nonmagnetic. The error in ΔH_{react} was estimated at 0.01-0.02 eV/formula unit. Hence our methodology establishes a link between the crystal structure that minimizes the energy and the battery potential $\overline{V}$. We can thus explore different structures and evaluate the ensuing potentials $\overline{V}$.

Results of Total Energy Calculations and Battery Voltages

$x_{Li} = 1$ and $x_{Li} = 0$.—We first present results for first-principles total energies, structural information, and intercalation energies (i.e., battery voltages) for (*i*) the fully lithiated stoichiometric $LiCoO_2$ compounds ($x = 1$) in the CuPt and D4 structures and (*ii*) the CuPt and D4 fully delithiated $\square CoO_2$ compounds ($x = 0$) formed by removal of Li from $LiCoO_2$, leaving a vacancy (denoted by $\square$), with subsequent atomic relaxation of the structural degrees of freedom. Figure 2 shows the energies of the structures considered, relative to $LiCoO_2$ and $\square CoO_2$ in the CuPt structure. (This choice of reference is merely for graphical purposes.)

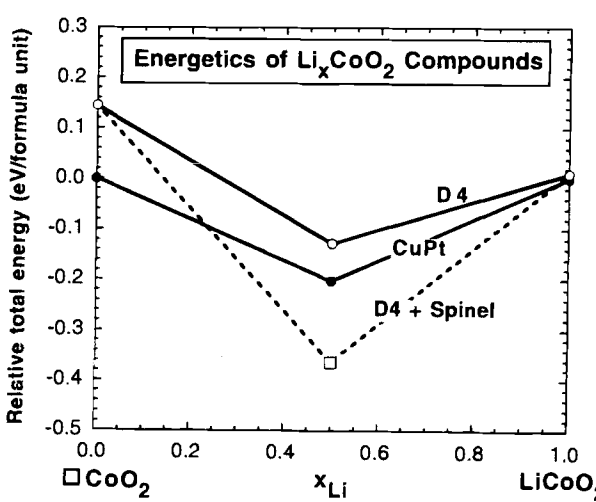

Fig. 2. LAPW calculated energetics of Li_xCoO_2 compounds in the CuPt, D4, and spinel structures. Energies (eV/Li_xCoO_2 formula unit) are shown relative to $xLiCoO_2 + (1 - x)\square CoO_2$ in the CuPt structure. The empty and filled circles connected by solid lines represent the energetics of symmetry-preserving removal of Li from the D4 (CuPt) structures, respectively. The empty square represents the energy of the $LiCo_2O_4$ spinel, and the dashed lines show the energetic pathway for symmetry-modifying removal of Li from the D4 structure. The average voltages of Eq. 2 are shown graphically as 3.78 V − m, where m is the slope of the various lines in this figure.

At $x = 1$, the structural energy difference (Fig. 2) between $LiCoO_2$ in the CuPt and D4 structures is very small (~0.01 eV/4 atom or 0.23 kcal/mol). This near degeneracy has been explained[30] in terms of the equivalence of pair- and three-body atom-atom correlation functions which measure the sequence of cation coordination shells in the two structures. The four-body atom-atom correlation, which breaks the degeneracy of CuPt and D4, is small and leads to the small energy difference between the two structures. The structural relaxation of the two phases is given in terms of their cell-internal parameters z, and for CuPt, the cell-external distortion δ. Structural relaxation of the two compounds gives calculated (measured, Ref. 5) values of $z = 0.262$ (0.264) and $\delta = 0.99$ (1.02) for the layered CuPt phase and $z = 0.259$ (0.257, Ref. 11) for the cubic D4 phase. Thus, in CuPt the Li–O and Co–O bond lengths are 2.08 and 1.90 Å (2.07 and 1.94, Ref. 5), respectively, whereas in D4 they are 2.05 and 1.91 (2.06 and 1.95, Ref. 11).

At $x = 0$, the separation in energy between CuPt and D4 (Fig. 2) increases in $\square CoO_2$ compared to $LiCoO_2$, due to the symmetry of the phases: upon extraction of Li in the layered CuPt structure, the calculated c/a ratio decreases significantly from 4.84 at $x = 1$ to 4.36 at $x = 0$, a decrease of ~10%, compared to the experimentally observed[7] decrease in c/a of ~9%. The Co–O bond length decreases from 1.90 Å in $LiCoO_2$ (CuPt) to 1.85 Å in $\square CoO_2$ (CuPt). This strong structural distortion of c/a in $\square CoO_2$ provides a significant avenue for energy lowering in $\square CoO_2$ (CuPt). D4, on the other hand, has cubic symmetry, and hence the cell parameters of $\square CoO_2$ (D4) cannot distort in any preferred direction (Table I). Consequently, $\square CoO_2$ (D4) does not relax as much as CuPt. The Co–O bond length in D4 decreases from 1.91 Å in $LiCoO_2$ to 1.85 Å in $\square CoO_2$ (D4). The similar decrease in Co–O bond length in the CuPt and D4 structures upon removal of Li is mostly due to the changes in the cell-internal parameter z rather than the c/a distortion which is present only in the CuPt structure. These differences in relaxation tendencies are important in comparing their intercalation energies, or average voltages.

We use Eq. 2 to compute average battery voltages for Li_xCoO_2 in the CuPt and D4 structures (Table II). The predicted average voltage of the layered $LiCoO_2$ structure

$$\overline{V}(\text{CuPt}, 1, 0) = 3.78 \text{ V} \quad [5]$$

is in good agreement with electrochemical measurements of $\overline{V} \sim 4.0 - 4.2$ V.[1,3,5,7] The ~10% difference between $\overline{V}$ of first-principles calculations and electrochemical experiments may be due to the local density approximation (LDA) used to treat the exchange and correlation terms of the total energy. Also, it has been speculated that this difference may arise from the overestimated cohesive energy of Li metal in LDA.[22] We also note that the intercalation voltage calculated in the manner described above is a bulk equilibrium quantity and does not contain contributions from the cathode surface, kinetic phenomena, or thermal entropies (the latter is expected to have only an extremely small effect on average voltage).[31]

The predicted intercalation energy from $x = 0$ to $x = 1$ is slightly larger in the cubic D4 structure

$$\overline{V}(\text{D4}, 1, 0) = 3.91 \text{ V} \quad [6]$$

Table II. Calculated average intercalation voltages $\overline{V}(\sigma, x_2, x_1)$ (Eq. 1 and 2) for Li_xCoO_2 in the structures σ = CuPt and D4.

	Layered CuPt Symmetry preserving	Cubic D4 Symmetry preserving	Cubic D4 Symmetry modifying
$\overline{V}(\sigma, 1, 0)$	3.78	3.91	3.91
$\overline{V}\left(\sigma, 1, \frac{1}{2}\right)$	3.37	3.50	3.04
$\overline{V}\left(\sigma, \frac{1}{2}, 0\right)$	4.19	4.32	4.78

than in layered CuPt. However, experimental reports[8-10] find a significantly lower voltage (by ~0.5 V) for cubic D4, compared with layered CuPt. We note that this discrepancy between calculated and observed voltage difference in layered and cubic $LiCoO_2$ is not likely to be due to the partial disorder of the low temperature cubic phase noted above. Recent first-principles calculations[30] have demonstrated the effect of cation disorder is to raise the average voltage slightly. Thus, a cubic phase with partial disorder is predicted to have an even higher average voltage than 3.91 V, thus widening the discrepancy between theory and experiment. However, these measured voltages of the cubic D4 phase are typically only for high Li compositions ($x_{Li} \geq 0.4$). We therefore study the intercalation energies and structural stability for intermediate ($x = 1/2$) Li compositions next.

$x_{Li} = 1/2$: symmetry-preserving Li removal.—In an attempt to reconcile this discrepancy between calculated, Eq. 6 and 5 and measured voltages of layered CuPt and cubic D4, we consider several "derivative" structures $Li_{0.5}CoO_2$ formed by partial removal of Li ($x = 1/2$) from the parent structures (CuPt or D4). First, we consider partially delithiated $x = 1/2$ structures formed by symmetry-preserving removal of Li from the parent structures. By symmetry-preserving Li removal, we mean removal of Li without changes in the positions of the remaining atoms (i.e., all atoms still octahedrally coordinated). We have computed the energetics of two $Li_{0.5}CoO_2$ compounds formed from CuPt and D4, respectively, by removing half of the Li atoms. All atomic positions are subsequently relaxed to their minimum energy positions (consistent with the symmetry of the structure). The CuPt-based $Li_{0.5}CoO_2$ structure (Fig. 1) considered is the ordered vacancy compound observed electrochemically by Reimers et al.[4] [See Fig. 2 of Reimers et al. for a figure of the (001) plane of the Li/□ ordered superlattice.] For the D4-based $Li_{0.5}CoO_2$ structure, we have simply chosen the only compound which corresponds to removing half the Li from D4 while not increasing the unit cell size (not shown in Fig. 1). The energies of these two symmetry-preserving $x = 1/2$ structures are shown in Fig. 2 as solid and empty circles. The energies of these structures are below the reference energy $xLiCoO_2 + (1 - x)\square CoO_2$ of their respective parent structures. This indicates that $Li_{0.5}\square_{0.5}CoO_2$ is stable against decomposition into $LiCoO_2 + \square CoO_2$, and hence that for the symmetry-preserving Li deintercalation from Li_xCoO_2 systems, ordered Li/□ compounds will be the low-energy ground states. This Li/□ ordering is probably a simple consequence of the electrostatic repulsion between the positively charged Li ions. Also, the stability of the CuPt-based $Li_{0.5}\square_{0.5}CoO_2$ phase is in agreement with the observations of Reimers et al.[4] in this system. The amount by which the energy of $Li_{0.5}CoO_2$ is below the end points is almost identical for the CuPt and D4 cases, that is, both $x = 1/2$ compounds are ~0.2 eV/formula unit below the average of their end point compounds. This equality implies that the Li/□ ordering tendency is relatively independent of cation structure.

By using Eq. 2, we may now compute the average voltages in two segments, from $x = 1$ to $x = 1/2$, and from $x = 1/2$ to $x = 0$. From Table II, one can see that the average voltage is lower for high Li contents than for low Li contents. However, removal of Li changes the voltages of the CuPt and D4 structures in an almost identical way (due to the similarity of Li/□ ordering tendencies) such that the voltage of the CuPt compound is still lower than D4 for each of the two segments. Thus, the symmetry-preserving removal of Li cannot explain the observed electrochemical differences between CuPt and D4.

$x_{Li} = 1/2$: symmetry-modifying Li removal.—We next explore the possibility of symmetry-modifying removal of Li from CuPt and D4 (i.e., deintercalation of Li accompanied by changes in positions of the remaining atoms). X-ray diffraction of the partially delithiated ($x_{Li} \sim 1/2$) Li_xCoO_2 cubic phase shows[16] the movement of (at least some) Li atoms from their octahedral sites in the D4 structure to the tetrahedral sites in the delithiated phase,[b] a spinel structure with stoichiometry $LiCo_2O_4 = 2Li_{1/2}CoO_2$. AB_2C_4 spinels generally exist in two varieties: normal and inverse (see Table III). In normal spinels, the one A (two B) atoms occupy tetrahedral (octahedral) sites, whereas in the inverse spinel, one A atoms occupies octahedral sites, but the B atoms are statistically distributed with half in octahedral and half in tetrahedral sites. The formation of the normal spinel $LiCo_2O_4$ structure (14 atoms/cell) from the $2LiCoO_2$ (=$Li_2Co_2O_4$) D4 structure (16 atoms/cell) can be imagined as follows: Co and O (12 atoms/cell) remain in the same octahedral sites as in D4, two of the Li atoms are removed, and the remaining two Li atoms move to the tetrahedral positions.[9,16] This is depicted graphically in Fig. 1 and structural information is given in Table III. Thus, whereas $x = 1$ D4 has Li and Co in octahedral O_h positions, the normal spinel structure has two Co in O_h positions, but Li in tetrahedral T_d sites. Table III contains a list of the octahedral/tetrahedral cation positions for all the structures considered. In addition to the calculations described above for octahedrally coordinated systems, we have also performed first-principles total energy calculations for the normal spinel $LiCo_2O_4$ structure (Fig. 2). We find that the normal spinel structure has a much lower energy than any of the other compounds calculated at $x = 1/2$, including $LiCoO_2 + CoO_2$ in the D4 structure. This low energy spinel suggests three conclusions

1. Upon extraction of one Li from the $Li_2Co_2O_4$ D4 phase it transforms into the $LiCo_2O_4$ normal spinel. Thus, one Li atom is removed and the other moves (from O_h to T_d sites) in order to form the low-energy normal spinel structure,

[b] One should note that Gummow et al.[9] removed Li from the D4 structure chemically (i.e., acid treatment), not electrochemically.

Table III. Cation positions (octahedral O_h vs. tetrahedral T_d) and relative energies for all Li_xCoO_2 structures considered. Octahedral (O_h) and Tetrahedral (T_d) sites indicate a cation coordinated by six and four oxygen atoms, respectively. The energy $\Delta E(\sigma)$ (eV/Li_xCoO_2 formula unit) of structure σ with respect to equivalent amounts of $LiCoO_2$ and $\square CoO_2$ is defined as $E(\sigma) - [xLiCoO_2(CuPt) + (1 - x)\square CoO_2(CuPt)]$. Also shown is the number of each cation type in octahedral/tetrahedral positions for the specified stoichiometry. The octahedral positions in the CuPt structure are denoted as O_h' to distinguish them from the octahedral positions in the D4 structure (denoted O_h). The distinction is due to the difference in unit-cell vectors between the two structures (Table I). The spinel structures (normal or inverse) have the same lattice vectors as the D4 structure (Table I), and thus the same octahedral positions. Thus, these positions are also labeled O_h.

x in Li_xCoO_2	Stoichiometry	Structure σ	Li	Co	$\Delta E(\sigma)$
1	$Li_2Co_2O_4$	CuPt	2 O_h'	2 O_h'	0.00
		D4	2 O_h	2 O_h	+0.01
1/2	$LiCo_2O_4$	CuPt	1 O_h'	2 O_h'	−0.20
		D4	1 O_h	2 O_h	−0.13
		Spinel-normal	1T_d	2 O_h	−0.36
		Spinel-inverse	1 O_h	1T_d + 1 O_h	+0.40
0	$\square_2Co_2O_4$	CuPt	—	2 O_h'	0.00
		D4	—	2 O_h	+0.14

but the Co and O atoms are not required to move in this transformation. One might ask, however, whether or not CuPt $Li_2Co_2O_4$ forms the normal spinel structure upon removal of one Li. This is much less likely, because both Li and Co atoms would have to change positions to form the normal spinel structure from CuPt: again, this transformation involves removal of one Li and one Li atom moving from O_h to T_d, however, some of the Co atoms would have to move substitutionally from Co O_h sites to Li O_h sites. The only way for Co atoms to make this movement would be to interrupt the close-packed oxygen sublattice. Thus, the formation of the $x = 1/2$ normal spinel from the $x = 1$ CuPt-based structure, while thermodynamically favored, is presumably kinetically inhibited.

2. The low energy of the normal spinel leads (via Eq. 2) to a significant reduction of the D4 average voltage from $x = 1$ to $x = 1/2$ (Table II), thus explaining the observed difference in voltage between CuPt and D4.[8,16,10] However, our calculations indicate that although the average voltage of the D4 structure is lower than CuPt down to $x = 1/2$, subsequent extraction of Li from the spinel structure corresponds to removal of Li from the (energetically favorable) T_d sites, and thus costs a large amount of energy. Thus, the average voltage of the D4 structure is predicted to rise sharply (4.78 V) from $x = 1/2$ to $x = 0$. Electrochemical measurements[8,16,10] of D4 have commonly probed only relatively high Li contents ($x \gtrsim 0.5$); however, Gummow et al.[16] have electrochemically extracted Li from the spinel $LiCo_2O_4$, observing a sharp increase in voltage (of ~1 V) near $x = 1/2$, in agreement with our calculations. If the capacity of Li extraction in the spinel phase $LiCo_2O_4$ could be improved, our calculations provide a prediction that this spinel would make a high voltage (4.78 V) battery cathode.

3. Because the spinel phase and the D4 are structurally distinct (i.e., Li is tetrahedrally coordinated in the former but octahedrally coordinated in the latter), the D4 Li_xCoO_2 system presumably forms a two-phase mixture of spinel + D4 for values for x_{Li} between 1/2 and 1, (as opposed to tolerating a large off-stoichiometry in either of the phases, in other words, when one begins removing Li from D4, one forms small pockets of spinel embedded in the D4 matrix). A two-phase mixture corresponds to straight line (a tie-line) in energy vs. composition (the dashed line in Fig. 2). The voltage is proportional to the slope of the energy vs. composition curve, and hence for a two-phase mixture, the voltage is constant. This is consistent with the measured voltage curves for D4 (down to $x_{Li} = 1/2$), which show a nearly constant plateau at 3.6 V. Thus, most of the electrochemical distinctions between the layered CuPt and cubic D4 phases of $LiCoO_2$ are explained by the low-energy $LiCo_2O_4$ spinel.

Tetrahedral vs. octahedral site preference energies.—To examine the stability of the Li and Co atoms with respect to distortions from O_h to T_d sites, we have undertaken two additional calculations

1. *$LiCo_2O_4$ inverse spinel.*—Many stable AB_2O_4 spinel compounds fall into one of two categories: the so-called normal spinel (which we described above) or the "inverse" spinel. The inverse spinel is a structure in which A atoms are in the O_h sites, but B atoms are statistically distributed, half in the O_h sites and half in the T_d sites (Table III). We examined the possibility of $LiCo_2O_4$ forming an inverse spinel by constructing a 14 atom $LiCo_2O_4$ cell to mimic the inverse spinel: Li in O_h sites, half of the Co in O_h and half in T_d. This inverse spinel cell is very high in energy relative to the normal spinel. On the scale of Fig. 2, it is about +0.4 eV, which places it more than 0.7 eV higher than the normal spinel. The inverse spinel has a very different structural relaxation than the normal spinel: when Li and Co are both in octahedral positions (such as in CuPt or D4), the calculated Li–O bonds are longer than Co–O bonds (see last line of Table I). Relative to the inverse spinel, the normal spinel has the "long-bond" atoms (Li) in tetrahedral sites, and hence these atoms are much closer to oxygen. However, in the inverse spinel, the "short-bond" atoms are in the tetrahedral sites. Because the Co–O bond is already quite short (with Co in O_h sites), moving Co to T_d makes an extremely short Co–O distance in the inverse spinel structure, which is energetically unfavorable. The high energy of the inverse spinel relative to the normal spinel indicates that the Li atoms are energetically favored to move to the tetrahedral sites, but moving the Co atoms from the octahedral sites is highly unfavorable.

2. *Energy pathway between T_d and O_h sites.*—We have also mapped the energy of the $LiCo_2O_4$ phase as Li is continuously moved from the octahedral (0, 0, 0) positions to the tetrahedral (1/4, 1/4, 1/4) sites along the direct pathway (ξ, ξ, ξ). Along this transition, when Li is at the T_d sites, the structure corresponds to the $LiCo_2O_2$ normal spinel structure. When the Li is in the O_h sites, the structure is the $Li_{0.5}CoO_2$ phase described above formed by "symmetry-preserving" removal of Li from D4. The energetics along this pathway will indicate whether the octahedral site become unstable upon Li extraction from D4 so that Li simply "falls" into the tetrahedral sites without any energy barrier, or if there is an energy barrier between tetrahedral and octahedral positions, and if so, what the magnitude of the barrier is. These calculations are shown in Fig. 3. A small activation barrier does exist for Li diffusion between the O_h and T_d sites, so that the octahedral positions are metastable, not unstable. The magnitude of the energy barrier (~0.07 eV) corresponds to $\exp(\delta E/kT) \sim 10^{-1}$ to 10^{-2} at room temperature. Thus, Li atoms attempting to cross this barrier (with roughly the Debye frequency) will easily do so on the time scale of seconds and move from octahedral to tetrahedral sites.

Results. Pressure-Induced Transitions

We have also searched for possible transition paths between the CuPt and D4 structures. Because CuPt and D4 are close in energy, and D4 has a smaller equilibrium volume than CuPt, one might suspect that a pressure-induced transition could exist between these two. Equations of state for the two phases are plotted in Fig. 4. We see that indeed the energy of D4 becomes lower than CuPt for positive pressures, with a transition pressure approximately 30 kbar. However, we should stress that because we have only con-

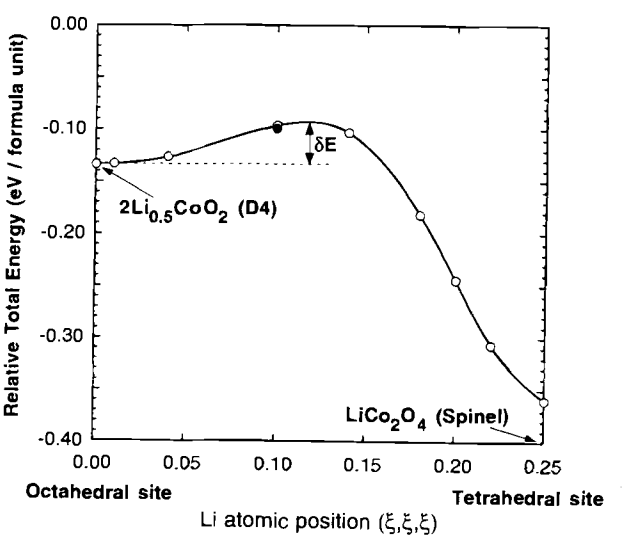

Fig. 3. Total energy of $LiCo_2O_4$ as the Li atoms are continuously distorted from the T_d sites (spinel) to the O_h sites ($x = 1/2$ D4) along the (ξ, ξ, ξ) path. Energies are shown (eV/Li_xCoO_2 formula unit) relative to $xLiCoO_2 + (1 - x)\square CoO_2$ in the CuPt structure. The barrier height δE is ~0.07 eV/Li atom. Co and O atoms are "frozen" in their relaxed positions in the $x = 1/2$ D4 structure. The filled circle shows a calculated point near the highest energy point where Co and O atoms are allowed to relax, demonstrating that the energy lowering from additional Co and O relaxation is minimal.

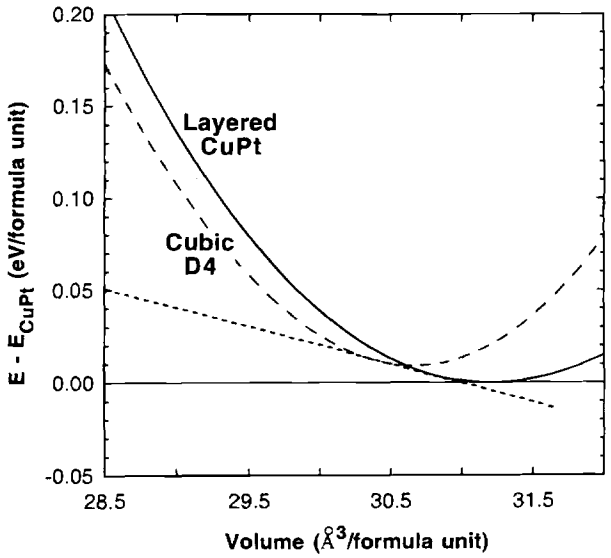

Fig. 4. Calculated equations of state for $LiCoO_2$ in the rhombohedral ("layered" or CuPt) and cubic (low temperature or D4) structures, shown as solid and dashed curves, respectively. The transition from CuPt to D4 can be seen at ~30 kbar (short dashed line).

sidered two possible end products, this calculation only demonstrates the possibility of a transition from CuPt to D4. In fact, there could be a pressure-induced transition from CuPt to some other phase. However, our calculations do clearly predict that a pressure-induced transition should occur (whether to the D4 phase or an even lower energy phase). It is noteworthy that the $LiVO_2$ compound, which is stable in the CuPt structure, has been synthesized in the D4 structure by high-pressure methods.[32] Also, we note that our calculations[30] indicate that the layered CuPt phase is the low temperature equilibrium form of $LiCoO_2$. The observed synthesis of the cubic phase at low temperature is therefore predicted to be a result of sluggish kinetics. The pressure-induced transition we have predicted here is an equilibrium transition, and thus is most likely to be observed at (high) temperatures where cation kinetics are fast enough to reach equilibrium (e.g., temperatures at which the layered phase is synthesized).

Conclusions

Using first-principles total energy calculations, we have investigated the structural stability, intercalation energies, and battery voltages of the two observed ordered phases (the layered CuPt and cubic D4 phases) of $LiCoO_2$. We have performed calculations for not only fully lithiated $LiCoO_2$, but also fully delithiated $\square CoO_2$ and partially delithiated (both symmetry-preserving and symmetry-modifying) $Li_{0.5}CoO_2$.

By examining the allowed structural distortions in the two structures, we find that the c/a ratio of $LiCoO_2$ (CuPt) is the only structural distinction between the otherwise similar CuPt and D4 phases. Because this c/a distortion is calculated to be very close to the ideal value in CuPt, the CuPt and D4 structures is $LiCoO_2$ are energetically nearly degenerate. However, upon removal of Li, the c/a ratio in $\square CoO_2$ (CuPt) decreases dramatically, whereas no such distortion occurs for $\square CoO_2$ (D4). Therefore, the energy difference between CuPt and D4 increases upon removal of Li.

We have examined the average voltages between various Li compositions for the CuPt and D4 structures. Because the two phases are nearly degenerate for $x = 1$, but not for $x = 0$, the voltage of Li_xCoO_2/Li cells averaged over all Li compositions, is larger for the cathode in the D4 structure compared with the CuPt structure, in apparent contrast with electrochemical measurements. To understand this apparent discrepancy, we undertook calculations of partially lithiated $x = 1/2$ compounds. We found that Li/□ ordering reduces the energy of symmetry-preserving (i.e., octahedrally coordinated Li) $Li_{0.15}CoO_2$ compounds by approximately equal amounts in layered CuPt and cubic D4, and thus does not explain the wide differences in observed voltages in the two materials. However, via symmetry-modifying removal of Li from D4, the Li atoms move from octahedral to tetrahedral sites and form the spinel compound, $LiCo_2O_4$. The low energy of this compound explains the low voltage of the D4 structure relative to CuPt (for $x \gtrsim 0.5$). In addition, for low Li compositions $0 < x < 0.5$, we predict that the average voltage of the D4 starting material should rise significantly upon removal of Li from the tetrahedral sites in $LiCo_2O_4$.

We have also investigated the stability of cations in the octahedral vs. tetrahedral sites. A small energy barrier is found to exist between Li in the T_d and O_h sites in $LiCo_2O_4$, thus demonstrating that the octahedral sites in the D4 phase are metastable, not unstable. In contrast to the energy gain of moving Li to T_d sites to form a normal spinel, formation of an inverse spinel by movement of the Co atoms to tetrahedral sites is shown to be highly energetically unfavorable. This large energetic cost of moving Co atoms also suggests that kinetic effects prohibit the Li_xCoO_2 CuPt phase from forming a spinel upon removal of Li.

Finally, we have pointed out a possible pressure-induced transition between the CuPt and D4 structures of $LiCoO_2$.

Acknowledgment

The authors gratefully acknowledge many helpful discussions with David Ginley, Jeanne McGraw, Phil Parilla, and John Perkins about the experimental aspects of this problem. Work at NREL was supported by the Office of Energy Research (OER) [Division of Materials Science of the Office of Basic Energy Sciences (BES)], U.S. Department of Energy, under contract no. DE-AC36-83CH10093.

Manuscript received January 20, 1998.

The National Renewable Energy Laboratory assisted in meeting the publication costs of this article.

REFERENCES

1. K. Mizushima, P. C. Jones, P. J. Wiseman, and J. B. Goodenough, *Mater. Res. Bull.*, **15**, 783 (1980).
2. T. A. Hewston and B. L. Chamberland, *J. Phys. Chem. Solids*, **48**, 97 (1987).
3. J. N. Reimers and J. R. Dahn, *J. Electrochem. Soc.*, **139**, 2091 (1992).
4. J. N. Reimers, J. R. Dahn, and U. von Sacken, *J. Electrochem. Soc.*, **140**, 2752 (1993).
5. T. Ohzuku, A. Ueda, M. Nagayama, Y. Iwakoshi, and H. Komori, *Electrochem. Acta*, **38**, 1159 (1993).
6. T. Ohzuku and A. Ueda, *J. Electrochem. Soc.*, **141**, 2972 (1994).
7. G. G. Amatucci, J. M. Tarascon, and L. C. Klein, *J. Electrochem. Soc.*, **143**, 1114 (1996).
8. R. J. Gummow and M. M. Thackeray, *Solid State Ionics*, **53**, 681 (1992).
9. R. J. Gummow, D. C. Liles, M. M. Thackeray, and W. I. F. David, *Mater. Res. Bull.*, **28**, 1177 (1993).
10. E. Rossen, J. N. Reimers, and J. R. Dahn, *Solid State Ionics*, **62**, 53 (1993).
11. M. Antaya, J. R. Dahn, J. S. Preson, E. Rossen, and J. N. Reimers, *J. Electrochem. Soc.*, **140**, 575 (1993).
12. K. A. Streibel, C. Z. Deng, S. J. Wen, and E. J. Cairns, *J. Electrochem. Soc.*, **143**, 1821 (1996).
13. G. G. Amatucci, J. M. Tarascon, D. Larcher, and L. C. Klein, *Solid State Ionics*, **84**, 169 (1996).
14. A. Zunger, in *Statics and Dynamics of Alloy Phase Transformations*, P. E. A. Turchi and A. Gonis, Editors, NATO ASI Series, Plenum, New York (1994).
15. M. Hansen and K. Anderko, *Constitution of Binary Alloys*, McGraw-Hill, New York (1958).
16. R. J. Gummow, D. C. Liles, and M. M. Thackeray, *Mater. Res. Bull.*, **28**, 235 (1993).
17. M. Antaya, K. Cearns, J. S. Preston, J. N. Reimers, and J. R. Dahn, *J. Appl. Phys.*, **76**, 2799 (1994).
18. B. Garcia, P. Barvoux, F. Ribot, A. Kahn-Harari, L. Mazerolles, and N. Baffier, *Solid State Ionics*, **80**, 111 (1995).
19. Z.-W. Lu, S.-H. Wei, A. Zunger, S. Frota-Pessoa, and L. G. Ferreira, *Phys. Rev. B*, **44**, 512 (1991).

20. W. Li, J. N. Reimers, and J. R. Dahn, *Phys. Rev. B*, **49**, 826 (1994).
21. J. N. Reimers and J. R. Dahn, *Phys. Rev. B*, **47**, 2995 (1993).
22. M. K. Aydinol, A. F. Kohan, G. Ceder, K. Cho, and J. Joannopoulos, *Phys. Rev. B*, **56**, 1354 (1997).
23. D. J. Singh, *Planewaves, Pseudopotentials, and the LAPW Method*, Kluwer, Boston, MA (1994).
24. *Solid State Batteries: Materials Design and Optimization*, C. Julien and G.-A. Nazri, Editors, Chap. 1, Kluwer, Boston, MA (1994).
25. P. Hohenberg and W. Kohn, *Phys. Rev. B*, **136**, 86 (1964).
26. W. Kohn and L. J. Sham, *Phys. Rev. A*, **140**, 1133 (1965).
27. D. M. Ceperley and B. J. Alder, *Phys. Rev. Lett.*, **45**, 566 (1980).
28. J. P. Perdew and A. Zunger, *Phys. Rev. B*, **23**, 5048 (1981).
29. S. Froyen, *Phys. Rev. B*, **39**, 3168 (1989).
30. C. Wolverton and A. Zunger, *Phys. Rev. B*, **57**, 2242 (1998).
31. E. Deiss, A. Wokaun, J.-L. Barras, C. Daul, and P. Dufek, *J. Electrochem. Soc.*, **144**, 3877 (1997).
32. C. Chieh, B. L. Chamberland, and A. F. Wells, *Acta Crystallogr.*, **B37**, 1813 (1981).

Gas Conversion Impedance: A Test Geometry Effect in Characterization of Solid Oxide Fuel Cell Anodes

S. Primdahl* and M. Mogensen*

Risø National Laboratory, Materials Research Department, 4000 Roskilde, Denmark

ABSTRACT

The appearance of an extra arc in impedance spectra obtained on high performance solid oxide fuel cell (SOFC) anodes is recognized when experiments are conducted in a test setup where the working and reference electrodes are placed in separate atmospheres. A simple continuously stirred tank reactor (CSTR) model is used to illustrate how anodes measured with the reference electrode in an atmosphere separate from the working electrode are subject to an impedance contribution from gas conversion. The gas conversion impedance is split into a resistive and a capacitive part, and the dependences of these parameters on gas composition, temperature, gas flow rate, and rig geometry are quantified. The fuel gas flow rate per unit of anode area is decisive for the resistivity, whereas the capacitance is proportional to the CSTR volume of gas over the anode. The model predictions are compared to actual measurements on Ni/yttria stabilized zirconia cermet anodes for SOFC. The contribution of the gas conversion overpotential to dc current-voltage characteristics is deduced for H_2/H_2O and shown to have a slope of $RT/2F$ in a Tafel plot.

Introduction

A detailed understanding of the rate-limiting steps in state-of-the-art Ni/YSZ cermet SOFC anodes is highly desirable from an optimization point of view. One of the most promising ways of unfolding such complex systems is by impedance spectroscopy. Here a number of more or less well separated arcs representing at least the same number of processes can be analyzed individually as a function of the primary test conditions.

Ni/YSZ cermet anodes for SOFC have been investigated intensively, and impedance spectra and interpretations of these have been offered in the literature.[1-10] The findings are surprisingly inconsistent, judging from the number of reported arcs in impedance spectra, even considering the different anode structures and test conditions applied. In this paper it is demonstrated how part of the disagreement may originate in the measurement setup rather than in the examined electrodes.

Considering a single electrode on an electrolyte (i.e., a half cell), the electrode overpotential $\eta_{\text{Electrode}}$ is given as the electrode potential $E(i)$ at current density i minus the equilibrium potential $E_{\text{Eq.}}$ (Nernst potential = zero current potential) corrected for the potential loss in the electrolyte of series resistance R_S

$$\eta_{\text{Electrode}} = E(i) - E_{\text{Eq.}} - iR_S \qquad [1]$$

This electrode overpotential is the summation of overpotentials of k rate-limiting processes in the electrode, Eq. 2. Processes like chemical reactions, charge transfer, and diffusion in the electrode are typically to be considered

$$\eta_{\text{Electrode}} = \sum_{\alpha=1}^{k} \eta_\alpha \qquad [2]$$

* Electrochemical Society Active Member.

One of the important assumptions in the above definitions is a sufficiently high flow rate of reactants to the cell to suppress concentration changes above the surface of the working electrode. It is the breakdown of this assumption which is examined below.

When a working electrode and a reference electrode are placed in different atmospheres, all electrochemical measurements involve the Nernst potential E, Eq. 3, between the oxygen partial pressures of these atmospheres

$$E = \frac{RT}{4F} \ln\left(\frac{x_{O_2,\text{red}}}{x_{O_2,\text{ox}}}\right) \qquad [3]$$

Here R, is the gas constant, T is the absolute temperature, and F is Faraday's constant. x_{O_2} refers to the mole fraction of O_2 in the reducing and oxidizing atmospheres, respectively. Variation in x_{O_2} in each of the compartments is a result of the gas flow rate per anode area, conversion by passing current, and gas mixing by diffusion, convection, and stirring. This phenomenon has already been considered and measured for dc loading of fuel cells.[11,12] The variation in the Nernst potential is inherent to the passage of current, and must be anticipated also in impedance measurements. It is here suggested to use the term gas-conversion impedance.

It is the aim of this paper to (*i*) draw attention to the presence of gas conversion impedance in SOFC research, and (*ii*) quantify the nature of gas conversion impedance and predict the ac and dc responses by introducing a simple CSTR model. Finally it is important to note how the presence of gas-conversion impedance is dependent on the measurement setup.

Experimental

Sample preparation.—A 40 to 50 μm thick Ni/YSZ cermet anode is prepared by spray painting. The ethanol based slurry is composed of green NiO and YSZ (Tosoh,